

Effect of new jet substructure measurements on Pythia8 tunes

Deepak Kar^a, Pratixan Sarmah^b

^aSchool of Physics, University of Witwatersrand
Johannesburg, South Africa.

Email: deepak.kar@cern.ch

^bDepartment of Physics, BITS Pilani
Rajasthan, India.

Email: pratixan123@gmail.com

Abstract

This masters project used the recent ATLAS jet substructure measurements to see if any improvements can be made to the commonly used Pythia8 Monash and A14 tunes.

Keywords:

Pythia8, jet substructure, FSR, tune

1. Introduction

The commonly used Pythia8 [1, 2] tunes, Monash [3] and A14 [4] are rather dated, and the latter was observed to have some tension with LEP measurements, primarily due to its lower Final State Radiation (FSR) α_s value. In last couple of years, a plethora of jet substructure [5, 6, 7, 8] measurements have been published by both ATLAS and CMS collaborations, utilising LHC Run 2 data. Here, we investigate the effect of four such ATLAS measurements on parameters sensitive to jet substructure observables.

2. Tuning setup

The following ATLAS measurements were considered in this study (along with their Rivet identifiers):

- Soft-Drop Jet Mass [9](ATLAS_2017_I1637587)
- Jet substructure measurements in multijet events [10] (ATLAS_2019_I1724098)
- Soft-drop observables [11](ATLAS_2019_I1772062)
- Lund jet plane with charged particles [12] (ATLAS_2020_I1790256)

The following parameters were considered in this tuning exercise, with the ranges stated in Table 1.

Parameter	Lower value	Upper value
BeamRemnants:primordialKThard	1.25	3
ColorReconnection:range	1.25	3
TimeShower:pTmin	0.5	1.5
MultipartonInteractions:pT0Ref	1.5	3
TimeShower:alphaSvalue	0.118	0.145

Table 1: Sampling range of the parameters considered

Weighted *hardQCD* events were generated with a *PThatMin* of 300 GeV. 100 Sampling runs were performed, each with 100000 events. Rivet3 [13] and Professor tuning system [14] were used. The goodness of sampling and the weight files used can be found in Appendix 5.2 and in Appendix 5.3.

3. Results

The first step was to ascertain where we have a scope of improvement. While a detailed observable-by-observable determination was performed (see Appendix 5.1), here we highlight the most salient features:

- For Lund Jet Plane (LJP) distributions, we observed that the hard-wide angle emissions part is better modelled by the Monash tune whereas the region ranging from UE/MPI to Soft-collinear and Collinear limits are in general better modelled by the A14 tune. However, this distributions also offer the biggest scope of improved modelling.
- For the soft drop ρ and r_g observables, in general Monash tune performs somewhat better than A14. One deviation from this trend is when the jet construction is Cluster based, in which case the A14 tune performs better over a large range.
- Both the Jet Substructure and Soft drop jet mass distributions are somewhat better modelled by the A14 tune.

Table 2 lists the parameter values of A14 and Monash along with our tuned values. A separate tune for LJP was performed as this analysis had the largest discrepancy. The LJP tune column shows the parameter values corresponding to the best tune for LJP and the Common Tune column shows the values of the best tune for all the analyses considered. Figures 1 and 2 show the tuned distributions for the one dimensional vertical slices of the LJP. Figure 3 shows the tuned distributions for the soft drop observables. Figure 4 shows the tuned distributions for soft drop mass. And lastly, Figure 5 shows the tuned distributions for the jet substructure observables.

Parameters	A14	Monash	LJP Tune	Common Tune
BeamRemnants:primordialKThard	1.88	1.8	2.288	2.065
ColorReconnection:range	1.71	1.8	2.73	1.69
TimeShower:pTmin	0.40	0.50	1.288	0.775
MultipartonInteractions:pT0Ref	2.09	2.28	2.766	2.91
TimeShower:alphaSvalue	0.127	0.1365	0.1308	0.1309

Table 2: Comparison of tuned values with Monash and A14

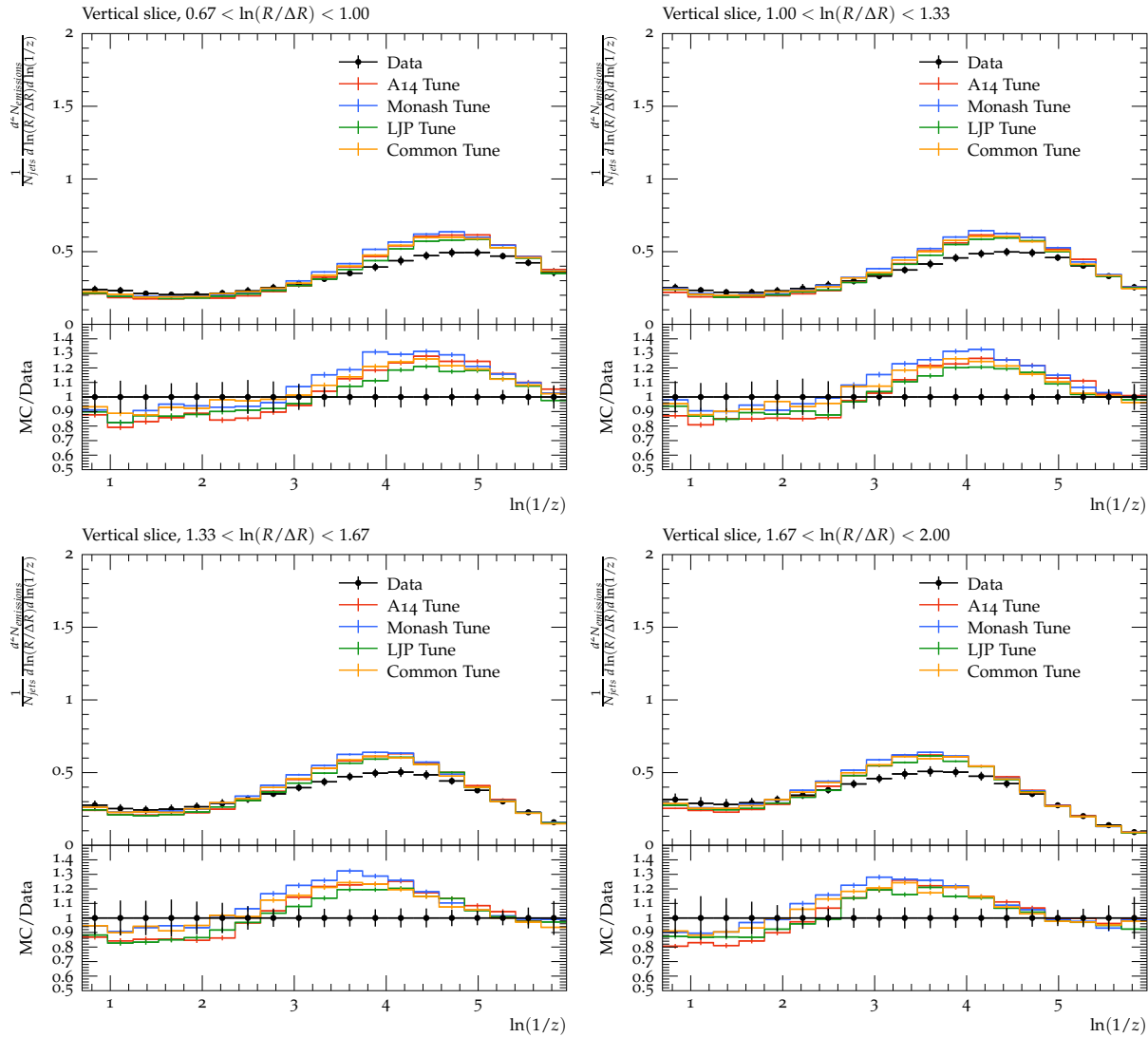


Figure 1: Comparison of our tunes with A14 and Monash tunes for Lund Jet Plane distributions (vertical slices)

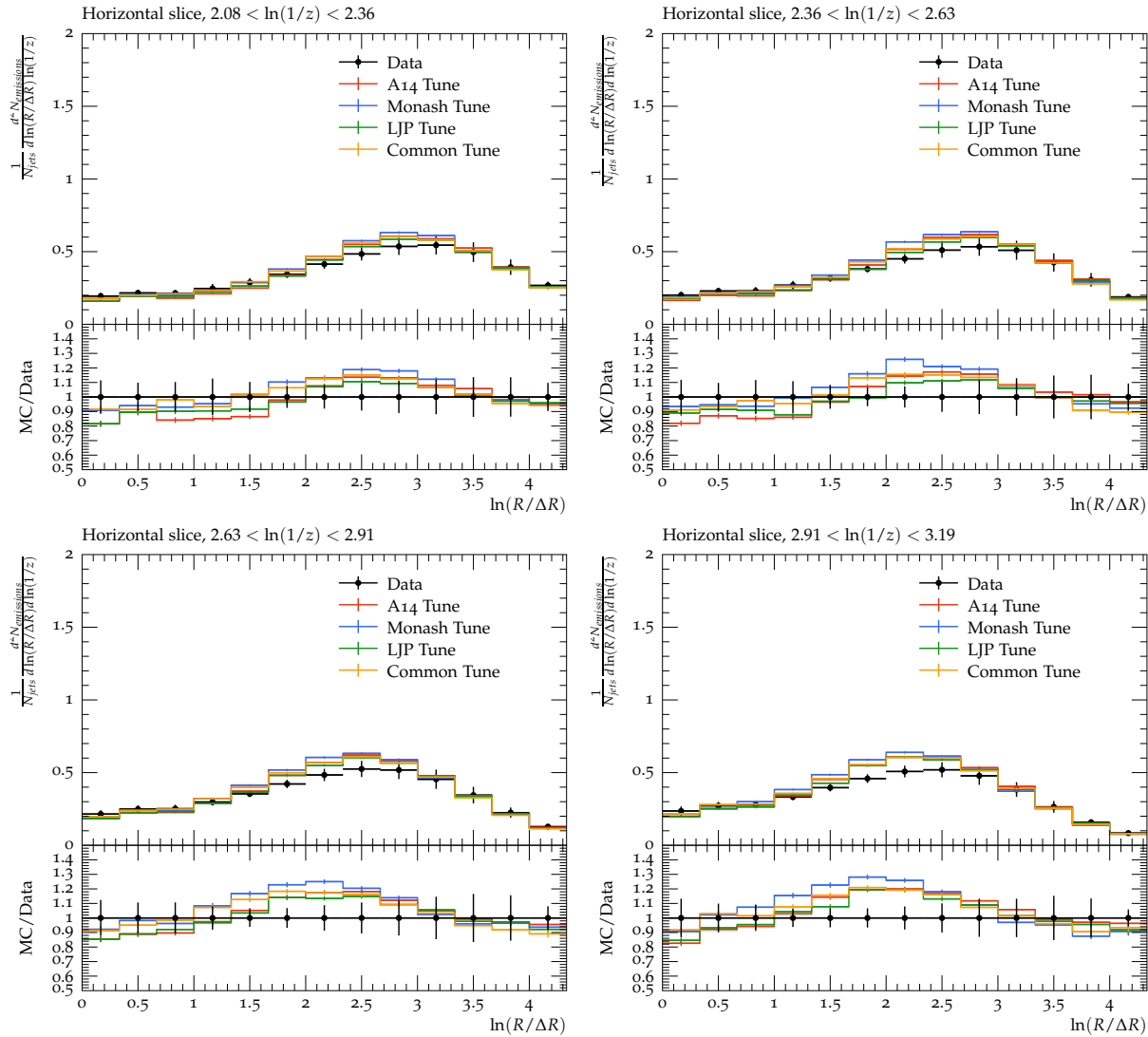


Figure 2: Comparison of our tunes with A14 and Monash tunes for Lund Jet Plane distributions (horizontal slices)

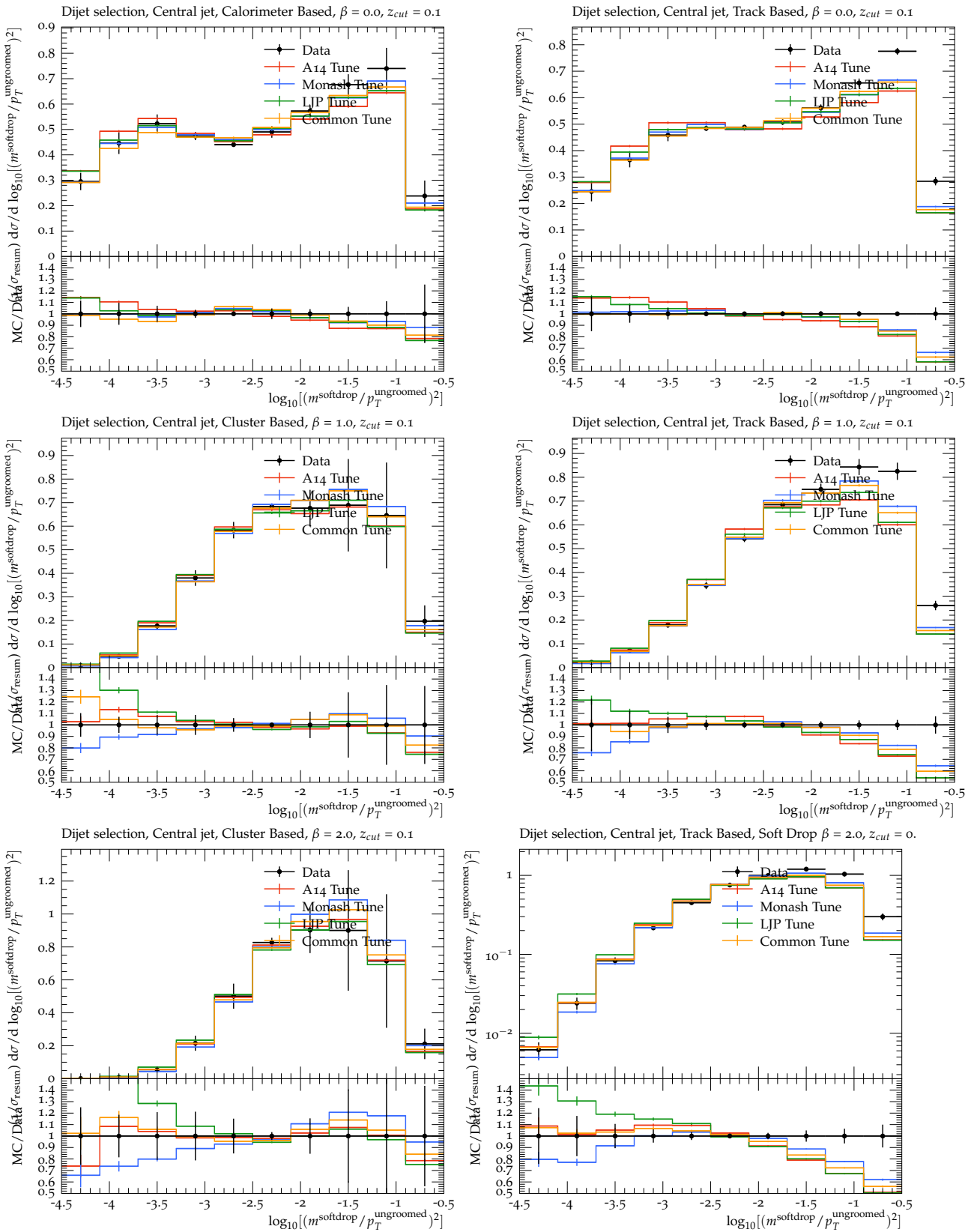


Figure 3: Comparison of our tunes with A14 and Monash tunes for soft drop jet mass distributions

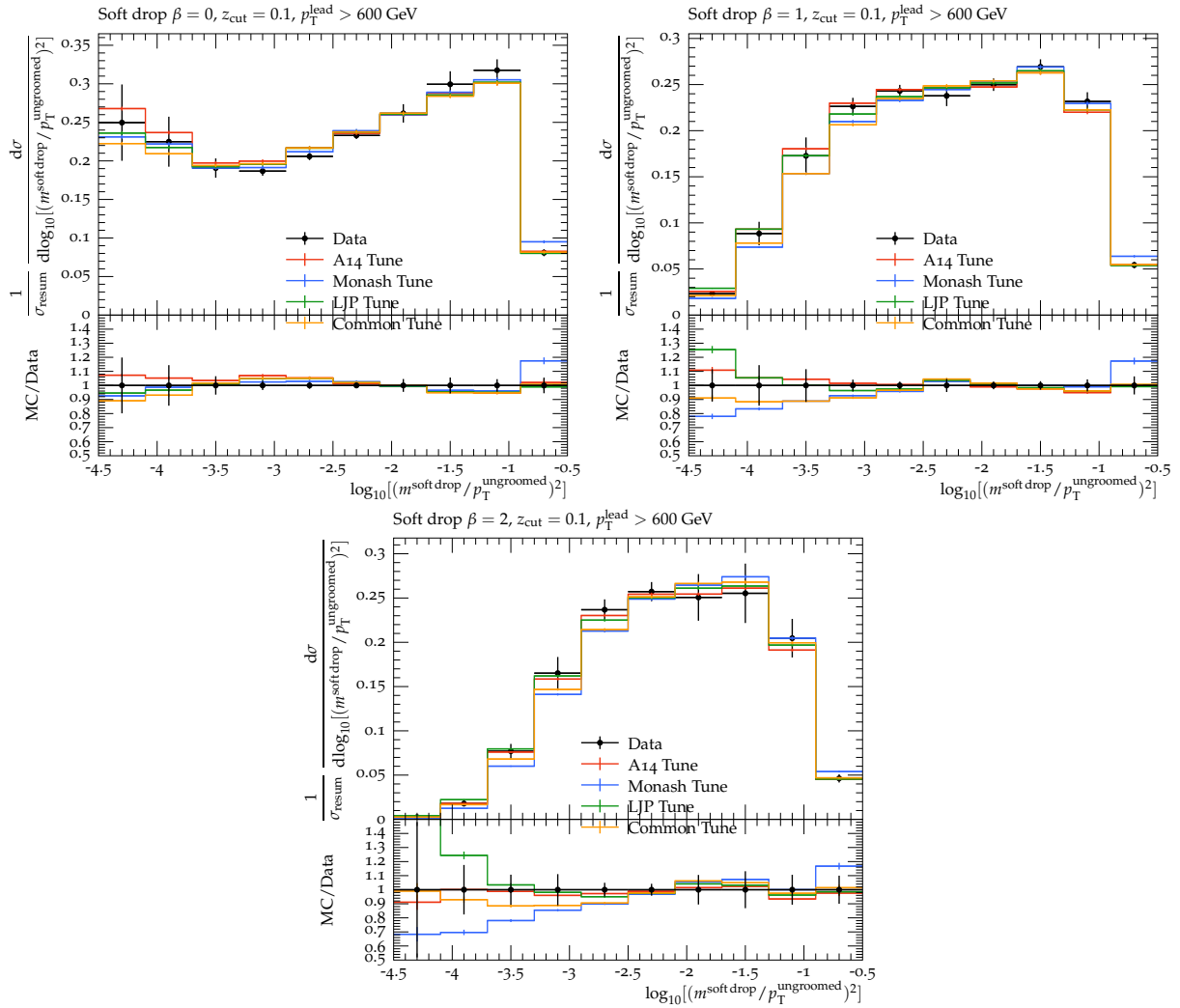


Figure 4: Comparison of our tunes with A14 and Monash tunes for soft drop jet mass distributions

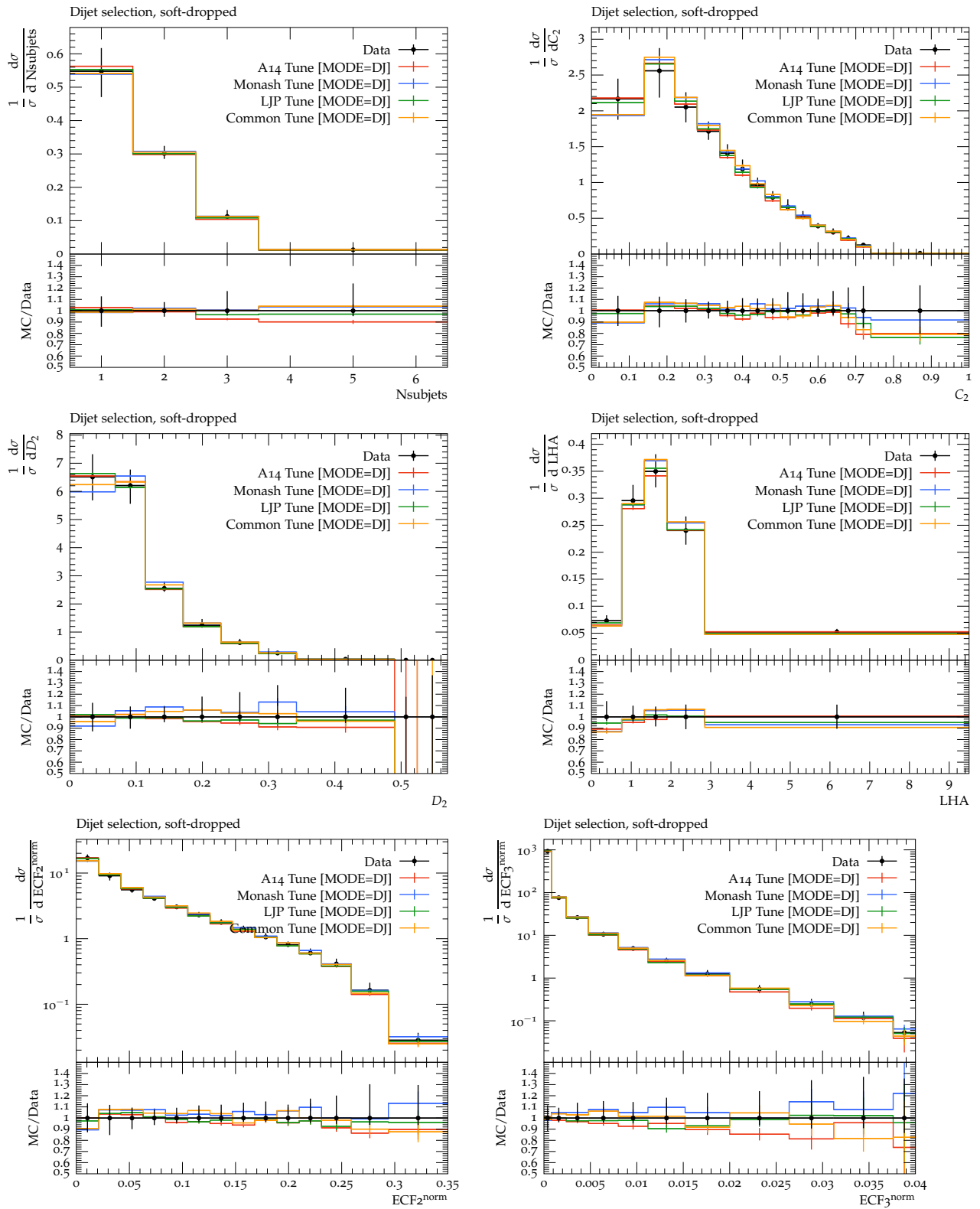


Figure 5: Comparison of our tunes with A14 and Monash tunes for jet Sub structure observable distribution for dijet selection

4. Summary

The results obtained show small improvements of roughly 5-10% in the distributions of the Lund Jet Plane and Soft Drop Mass distributions from the previous A14 and Monash Tunes. As in Table 2, it can be seen that the parameter values of the tunes obtained are pulled up from the A14 and Monash Tunes. In the case of the LJP , we see that the A14 and Monash Tunes deviate most from the data near the peaks of the distributions. This is the region where soft collinear effects transitions to UE/MPI effects in the LJP. Since the tunes we obtained improve this region of the distributions, it can be inferred that higher values of these parameters facilitate more soft radiations in the final state.

In the case of the soft drop observable distributions, there are regions that require generation of more mass to model the data better. These compete with the LJP values and decreases values of parameters: *BeamRemnants:primordialKTHard* from 2.288 to 2.065, *ColorReconnection:range* from 2.73 to 1.69, *TimeShower:pTmin* from 1.288 to 0.775. For the other two parameters, *MPI:pT0Ref* and *TimeShower:alphaSvalue*, the values increased slightly.

Acknowledgements

DK is funded by National Research Foundation (NRF), South Africa through Competitive Programme for Rated Researchers (CPRR), Grant No: 118515. We thank Andy Buckley and Holger Schulz for technical assistance with Professor program, as well as for physics discussions.

References

- [1] T. Sjostrand, S. Mrenna, P. Z. Skands, A Brief Introduction to PYTHIA 8.1, *Comput. Phys. Commun.* 178 (2008) 852–867. [arXiv:0710.3820](https://arxiv.org/abs/0710.3820), doi:10.1016/j.cpc.2008.01.036.
- [2] T. Sjöstrand, S. Ask, J. R. Christiansen, R. Corke, N. Desai, P. Ilten, S. Mrenna, S. Prestel, C. O. Rasmussen, P. Z. Skands, An Introduction to PYTHIA 8.2, *Comput. Phys. Commun.* 191 (2015) 159–177. [arXiv:1410.3012](https://arxiv.org/abs/1410.3012), doi:10.1016/j.cpc.2015.01.024.
- [3] P. Skands, S. Carrazza, J. Rojo, Tuning PYTHIA 8.1: the Monash 2013 Tune, *Eur. Phys. J. C* 74 (8) (2014) 3024. [arXiv:1404.5630](https://arxiv.org/abs/1404.5630), doi:10.1140/epjc/s10052-014-3024-y.
- [4] ATLAS Collaboration, ATLAS Pythia 8 tunes to 7 TeV data, ATL-PHYS-PUB-2014-021 (2014). URL <https://cds.cern.ch/record/1966419>
- [5] A. Altheimer, et al., Jet Substructure at the Tevatron and LHC: New results, new tools, new benchmarks, *J. Phys. G* 39 (2012) 063001. [arXiv:1201.0008](https://arxiv.org/abs/1201.0008), doi:10.1088/0954-3899/39/6/063001.
- [6] A. Altheimer, et al., Boosted objects and jet substructure at the LHC. Report of BOOST2012, held at IFIC Valencia, 23rd-27th of July 2012, *Eur. Phys. J. C* 74 (3) (2014) 2792. [arXiv:1311.2708](https://arxiv.org/abs/1311.2708), doi:10.1140/epjc/s10052-014-2792-8.
- [7] S. Marzani, G. Soyez, M. Spannowsky, Looking inside jets: an introduction to jet substructure and boosted-object phenomenology, Vol. 958, Springer, 2019. [arXiv:1901.10342](https://arxiv.org/abs/1901.10342), doi:10.1007/978-3-030-15709-8.
- [8] R. Kogler, et al., Jet Substructure at the Large Hadron Collider: Experimental Review, *Rev. Mod. Phys.* 91 (4) (2019) 045003. [arXiv:1803.06991](https://arxiv.org/abs/1803.06991), doi:10.1103/RevModPhys.91.045003.
- [9] ATLAS Collaboration, Measurement of the Soft-Drop Jet Mass in pp Collisions at $\sqrt{s} = 13$ TeV with the ATLAS Detector, *Phys. Rev. Lett.* 121 (9) (2018) 092001. [arXiv:1711.08341](https://arxiv.org/abs/1711.08341), doi:10.1103/PhysRevLett.121.092001.
- [10] ATLAS Collaboration, Measurement of jet-substructure observables in top quark, W boson and light jet production in proton-proton collisions at $\sqrt{s} = 13$ TeV with the ATLAS detector, *JHEP* 08 (2019) 033. [arXiv:1903.02942](https://arxiv.org/abs/1903.02942), doi:10.1007/JHEP08(2019)033.
- [11] ATLAS Collaboration, Measurement of soft-drop jet observables in pp collisions with the ATLAS detector at $\sqrt{s} = 13$ TeV, *Phys. Rev. D* 101 (5) (2020) 052007. [arXiv:1912.09837](https://arxiv.org/abs/1912.09837), doi:10.1103/PhysRevD.101.052007.
- [12] ATLAS Collaboration, Measurement of the Lund Jet Plane Using Charged Particles in 13 TeV Proton-Proton Collisions with the ATLAS Detector, *Phys. Rev. Lett.* 124 (22) (2020) 222002. [arXiv:2004.03540](https://arxiv.org/abs/2004.03540), doi:10.1103/PhysRevLett.124.222002.

- [13] C. Bierlich, et al., Robust Independent Validation of Experiment and Theory: Rivet version 3, *SciPost Phys.* 8 (2020) 026. [arXiv:1912.05451](https://arxiv.org/abs/1912.05451), doi:10.21468/SciPostPhys.8.2.026.
- [14] A. Buckley, H. Hoeth, H. Lacker, H. Schulz, J. E. von Seggern, Systematic event generator tuning for the LHC, *Eur. Phys. J. C* 65 (2010) 331–357. [arXiv:0907.2973](https://arxiv.org/abs/0907.2973), doi:10.1140/epjc/s10052-009-1196-7.

5. Appendix

5.1. Tune performance

Plots	Observable	$\ln(R/\Delta R)$ or $\ln(1/z)$ Slice	Better Tune Performance regions		Better Tune (overall) (Monash)
			A14	Monash	
d03-x01-y01	$\ln(1/z)$	0.00-0.33	4.3-6	0.7-4.3	Monash
d04-x01-y01	$\ln(1/z)$	0.33-0.67	3.4-4.2	0.7-3.4, 4.4-6	Monash
d05-x01-y01	$\ln(1/z)$	0.67-1.00	3-5	0.7-3, 5-6	Monash
d06-x01-y01	$\ln(1/z)$	1.00-1.33	3-4.2	0.7-3, 4.2-6	Monash
d07-x01-y01	$\ln(1/z)$	1.33-1.67	2.4-4.2	0.7-2.4, 4.3-6	Monash
d08-x01-y01	$\ln(1/z)$	1.67-2.00	2-4, 5.2, 5.8	0.7-2, 4-5, 5.5	-
d09-x01-y01	$\ln(1/z)$	2.00-2.33	1.8-4, 4.7, 5.2-6	0.7-1.8, 4-4.4	A14
d10-x01-y01	$\ln(1/z)$	2.33-2.67	1.6-3, 4.4-5.8	0.7-1.4, 3.2-4.2	A14
d11-x01-y01	$\ln(1/z)$	2.67-3.00	1.4-5	0.7-1.2, 5.2-5.8	A14
d12-x01-y01	$\ln(1/z)$	3.00-3.33	0.8-1.4, 3-4, 4.7, 5.8	1.6-3, 3.3, 4-4.5, 5-5.6	-
d13-x01-y01	$\ln(1/z)$	3.33-3.67	0.7-3.4, 4.6-5	3.6-4.4, 5.1-6	A14
d14-x01-y01	$\ln(1/z)$	3.67-4.00	0-3.4	3.6-4.6	A14
d15-x01-y01	$\ln(1/z)$	4.00-4.33	0.7-2.6, 3.6, 4-4.6, 5, 5.57	2.7-3.4, 3.9, 4.7, 5.23	A14
d16-x01-y01	$\ln(R/\Delta R)$	0.69-0.97	3-4.5	0-3	Monash
d17-x01-y01	$\ln(R/\Delta R)$	0.97-1.25	3-4	0-3	Monash
d18-x01-y01	$\ln(R/\Delta R)$	1.25-1.52	2.7-3.2, 3.5-4	0-2.6	Monash
d19-x01-y01	$\ln(R/\Delta R)$	1.52-1.80	2.4-4.5	0.5-2.3	-
d20-x01-y01	$\ln(R/\Delta R)$	1.80-2.08	2-3, 3.3-4.5	0-2	-
d21-x01-y01	$\ln(R/\Delta R)$	2.08-2.36	1.6-4.5	0-1.6, 2.2, 3.4-4	-
d22-x01-y01	$\ln(R/\Delta R)$	2.36-2.63	1.4-3, 3.6-4.5	0-1.3, 3-3.6	A14
d23-x01-y01	$\ln(R/\Delta R)$	2.63-2.91	1.4-3, 3.5	0-1.3, 3-4.5	-
d24-x01-y01	$\ln(R/\Delta R)$	2.91-3.19	0.6-4.5	0-0.5	A14
d25-x01-y01	$\ln(R/\Delta R)$	3.19-3.47	0.6-2.4, 3.4-4.5	0-0.5, 2.4-3.3	A14
d26-x01-y01	$\ln(R/\Delta R)$	3.47-3.74	0.5-4.5	0.2, 1.2, 2.5, 3.5	A14
d27-x01-y01	$\ln(R/\Delta R)$	3.74-4.02	0.3-4.5	0.2	A14
d28-x01-y01	$\ln(R/\Delta R)$	4.02-4.30	0-1.6, 3.7-4.5	1.7-3.6	-
d29-x01-y01	$\ln(R/\Delta R)$	4.30-4.57	0.2, 0.5, 1.2, 2.3-4.5,	0.8, 1-2.2, 3.2, 3.8	-
d30-x01-y01	$\ln(R/\Delta R)$	4.57-4.85	0.2, 1.6-3.3, 3.5	0.3-1.5, 3.7-4.5	-
d31-x01-y01	$\ln(R/\Delta R)$	4.85-5.13	0-3, 3.4-4.5	3.2	A14
d32-x01-y01	$\ln(R/\Delta R)$	5.13-5.41	0.2, 1.7-4	0.4-1.7, 2.75	A14
d33-x01-y01	$\ln(R/\Delta R)$	5.41-5.68	0.2, 2-3	0.5-2, 3.2-4	Monash
d34-x01-y01	$\ln(R/\Delta R)$	5.68-5.96	1.7-2.3	0-1.7, 2.5-3	Monash

Table 3: ATLAS_2020_I1790256(LJP)

Plots		β	z_{cut}	Observable	A14	Monash	Better Tune
d01-x01-y01	Calorimeter based	0	0.1	ρ	-	all	Monash
d02-x01-y01	Track based	0	0.1	ρ	-	all	Monash
d03-x01-y01	Cluster based	1	0.1	ρ	[-4.5,-3.7], [-2,-1.3]	[-3.5,-2.1], [-1,-0.5]	A14/ Monash
d04-x01-y01	Track based	1	0.1	ρ	[-4.5,-3.7]	[-3.5,-0.5]	Monash
d05-x01-y01	Cluster based	2	0.1	ρ	[-4.5,-1.1]	-0.7	A14
d06-x01-y01	Track based	2	0.1	ρ	[-4.5,-3.7]	[-3.5,-0.5]	Monash
d07-x01-y01	Track based	1	0.1	ρ	[-4.5,-3.7]	[-3.5,-0.5]	Monash
d16-x01-y01	Track based	1	0.1	r_g	-	all	Monash
d17-x01-y01	Cluster based	2	0.1	r_g	[-1.2,-0.2]	-0.15	A14
d18-x01-y01	Track based	2	0.1	r_g	-1.1	[-1,-0.1]	Monash
d19-x01-y01	Central jet/Calorimeter	0	0.1	r_g	-	all	Monash
d20-x01-y01	Central jet/Track	0	0.1	r_g	-	all	Monash
d21-x01-y01	Central jet/Cluster	1	0.1	ρ	[-4.5,-1]	-0.7	A14
d22-x01-y01	Central jet/Track	1	0.1	ρ	[-4.5,-3.7]	[-3.5,-0.5]	Monash
d23-x01-y01	Central jet/Cluster	2	0.1	ρ	[-3.5,-0.9]	-0.7	A14
d24-x01-y01	Central jet/Track	2	0.1	ρ	[-4.5,-3.7]	[-3.5,-0.7]	Monash
d34-x01-y01	Central jet/Track	1	0.1	r_g	-	all	Monash
d35-x01-y01	Central jet/Cluster	2	0.1	r_g	[-1.2,-0.4]	-0.5,-0.15	A14
d36-x01-y01	Central jet/Track	2	0.1	r_g	-1.1	[-1,-0.1]	Monash
d37-x01-y01	Forward jet/Calorimeter	0	0.1	r_g	-	all	Monash
d38-x01-y01	Forward jet/Track	0	0.1	ρ	-	all	Monash
d39-x01-y01	Forward jet/Cluster	1	0.1	ρ	-4.3	[-4,-0.5]	Monash
d40-x01-y01	Forward jet/Track	1	0.1	ρ	[-4.5,-3.7]	[-3.5,-0.5]	Monash
d41-x01-y01	Forward jet/Cluster	2	0.1	ρ	-3.9,[-3.1,-1]	-3.5,-0.7	A14
d42-x01-y01	Forward jet/Track	2	0.1	ρ	[-4.5,-3.7]	[-3.5,-0.5]	Monash
d49-x01-y01	Forward jet/Track	0	0.1	r_g	all	all	-
d51-x01-y01	Forward jet/Cluster	1	0.1	r_g	[-0.8,-0.2]	[-1.2,-0.8],-0.1	-
d52-x01-y01	Forward jet/Track	1	0.1	r_g	-	all	Monash
d53-x01-y01	Forward jet/Cluster	2	0.1	r_g	all	-0.15	A14
d54-x01-y01	Forward jet/Track	2	0.1	r_g	-1.1	[-1,-0.1]	Monash

Table 4: ATLAS 2019 I1772062(Soft_Drop_Jet Observables)

Plots	Observable	Better Tune Performance regions		Better Tune (overall)
		A14	Monash	
d01-x01-y01	Nsubjets	0-10	-	A14
d02-x01-y01	C_2	0-0.86	0.36-0.42 , 0.64-0.72	A14
d03-x01-y01	D_2	0-0.5	-	A14
d04-x01-y01	LHA	0.45	-	A14
d05-x01-y01	ECF_2^{norm}	0-0.252	0.252-0.35	A14
d06-x01-y01	ECF_3^{norm}	0-0.04	-	A14
d23-x01-y01	Nsubjets	1-2	2-5	Monash
d24-x01-y01	C_2	0-0.38 , 0.42-0.5 , 0.54-0.62	0.4 , 0.52 , 0.62-1.0	A14
d25-x01-y01	D_2	0-0.48	-	A14
d26-x01-y01	LHA	0-1.4	1.4-9	A14
d27-x01-y01	ECF_2^{norm}	0-0.23	ECF_2^{norm} 0.23-0.35	A14
d28-x01-y01	ECF_3^{norm}	0-0.02	0.02-0.32	A14

Table 5: ATLAS 2019 I1724098(JSS, Dijet Selection)

Plots	Observable ($p_T^{lead} > 600 \text{ GeV}$)	β ($z_{cut} = 0.1$)	Better Tune Performance regions		Better Tune (overall)
			A14	Monash	
d01-x01-y01	$\log_{10}[(m^{\text{soft drop}} / p_T^{\text{ungroomed}})^2]$	0	[-2.5,-0.5]	[-4,-2.5]	A14
d02-x01-y01	$\log_{10}[(m^{\text{soft drop}} / p_T^{\text{ungroomed}})^2]$	1	[-4.5,-0.5]	-	A14
d03-x01-y01	$\log_{10}[(m^{\text{soft drop}} / p_T^{\text{ungroomed}})^2]$	2	[-4.5,-0.5]	-	A14

Table 6: ATLAS 2017 I1637587(Soft Drop Mass)

5.2. Envelope plots

Having decided the range of values for each parameter, we visualise the region of the distributions to check its utility and hence it is important before proceeding further. This can be done using the PROFESSOR tool by generating envelopes plots with the command `prof2-envelopes`. The envelope plots show an area covering the distributions which indicates the bin values that the observables can take within the selected parameter ranges. These are shown in the following sub sections.

5.2.1. Soft Drop Mass Distributions

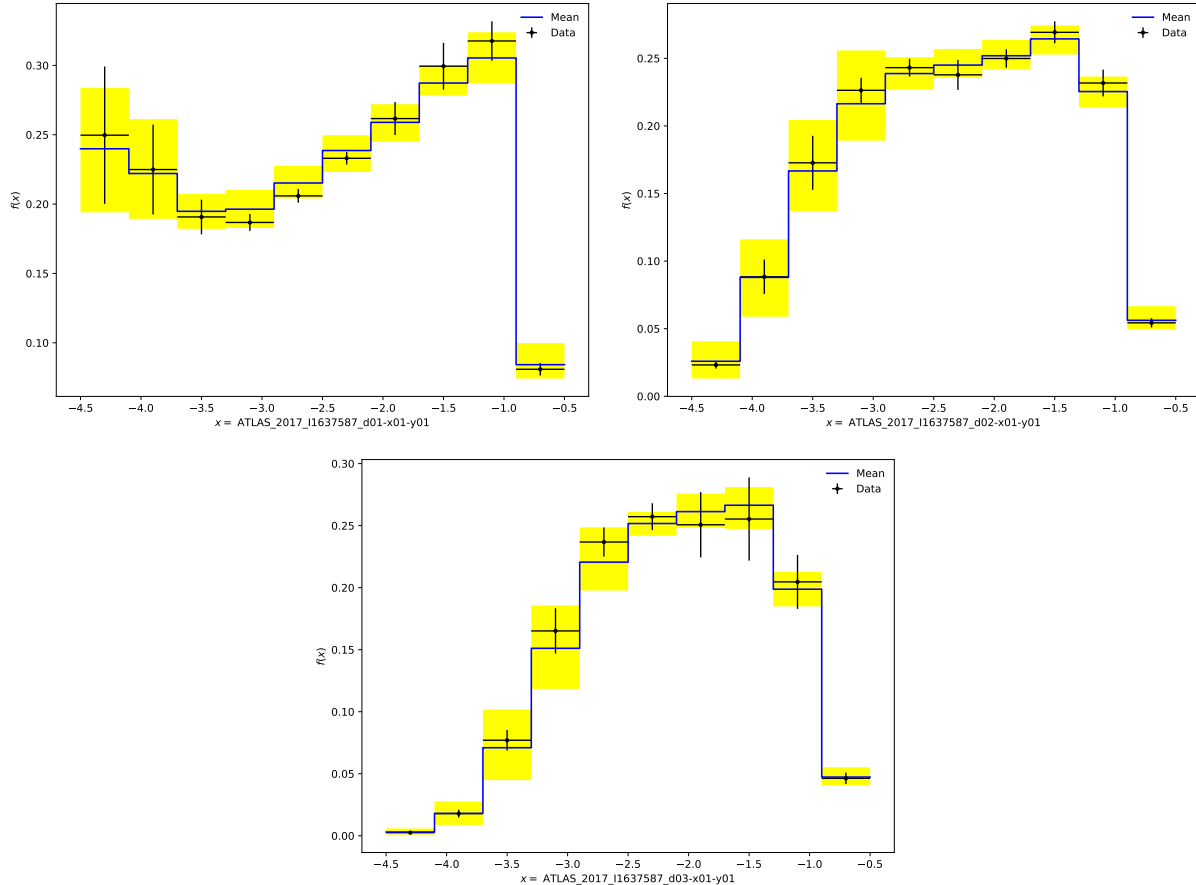


Figure 6: Envelope plots for ATLAS_2017_I1637587

As can be seen in Figure 6, The envelopes cover the reference data in almost every bin and hence we can say that the range selected for the parameters are appropriate.

5.2.2. Lund Jet Plane Distributions

As can be seen in Figure 7, the envelopes do not entirely cover the reference data. This is because we have reached a limit as to how much the distribution can be further fitted to the data with Pythia. Thus we consider this suitable for the purpose of this report and proceed with our set of parameter ranges.

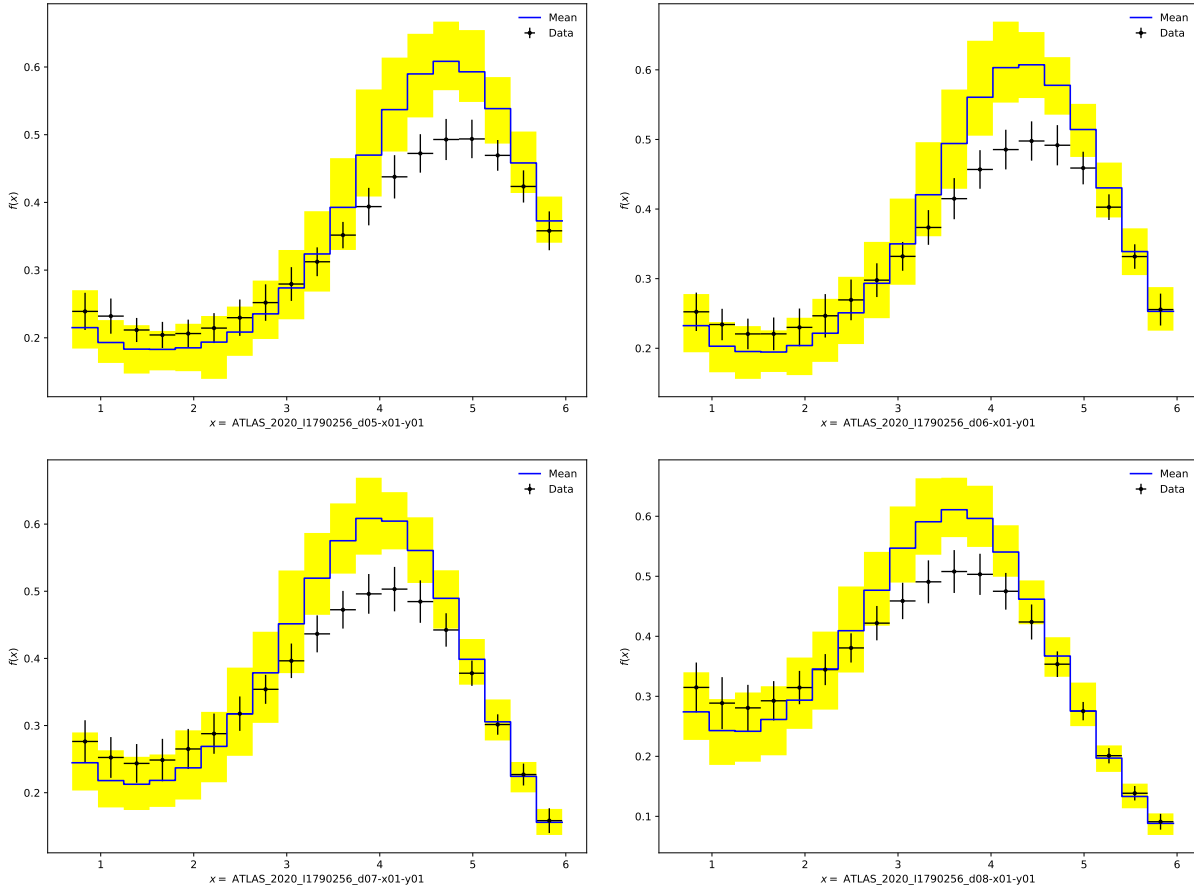


Figure 7: Envelope plots for Lund Jet Plane

5.2.3. Soft Drop Observables Distributions

In the Figure 8, we see that the envelopes cover the data points in almost all the bins of our distributions of interest i.e soft drop jet mass from the soft drop jet observables analysis. Thus the parameter ranges are suitable for proceeding to tune the distributions.

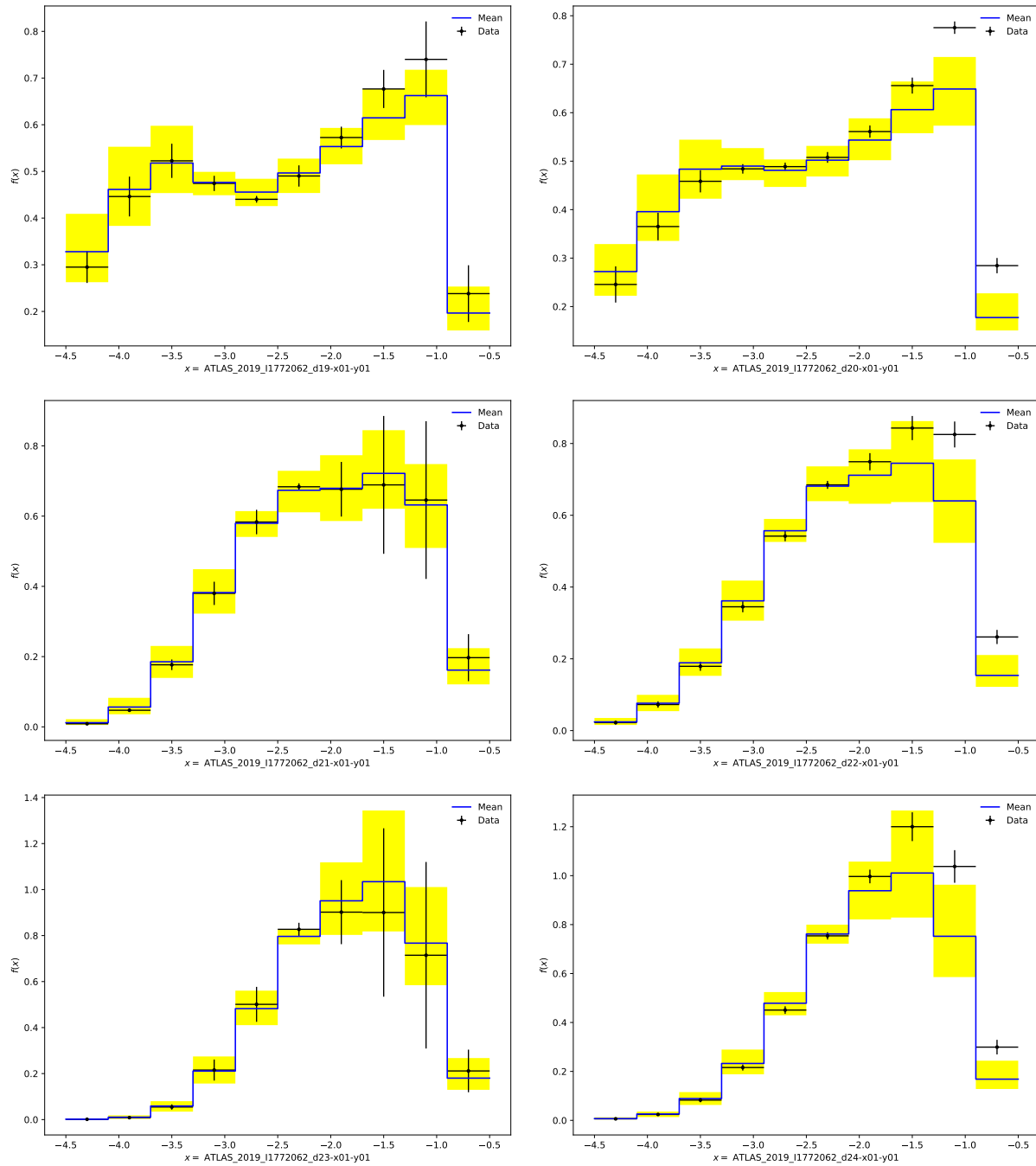


Figure 8: Envelope plots for Soft Drop Mass observable

5.3. Weight file

The weight file assigns weights to the distributions to be tuned and hence is manually changed depending on our interests. For this project, a total of 16 distributions were assigned weights greater than 1 and 6 distributions were given no weight i.e 0 for obtaining the Common Tune. These are :

Analysis	Distribution code	Weight
ATLAS_2020_I1790256	d03-x01-y01	106
ATLAS_2020_I1790256	d04-x01-y01	112
ATLAS_2020_I1790256	d05-x01-y01	108
ATLAS_2020_I1790256	d06-x01-y01	20
ATLAS_2020_I1790256	d07-x01-y01	16.6
ATLAS_2020_I1790256	d08-x01-y01	16
ATLAS_2020_I1790256	d09-x01-y01	16
ATLAS_2019_I1772062	d19-x01-y01	75
ATLAS_2019_I1772062	d20-x01-y01	75
ATLAS_2019_I1772062	d21-x01-y01	200
ATLAS_2019_I1772062	d22-x01-y01	80
ATLAS_2019_I1772062	d23-x01-y01	200
ATLAS_2019_I1772062	d24-x01-y01	80
ATLAS_2017_I1637587	d01-x01-y01	500
ATLAS_2017_I1637587	d02-x01-y01	500
ATLAS_2017_I1637587	d03-x01-y01	500
ATLAS_2019_I1772062	d61-x01-y01	0
ATLAS_2019_I1772062	d62-x01-y01	0
ATLAS_2019_I1772062	d79-x01-y01	0
ATLAS_2019_I1772062	d80-x01-y01	0
ATLAS_2019_I1772062	d97-x01-y01	0
ATLAS_2019_I1772062	d98-x01-y01	0

Table 7: Weights assigned to obtain the Common tune